




Development of Intensity-Duration-Frequency (IDF) Models for Manually Operated Rain Gauge Catchment: A Case Study of Port Harcourt Metropolis Using 50years Rainfall Data)

Francis J. Ogbozige *

Civil Engineering Dept, University of Federal Otuoke-Nigeria.

*Corresponding author Email: ogbozige@fuotuo.ke.edu.ng

HIGHLIGHTS

- The IDF curves were developed using Gumbel, Pearson type III, and Log-Pearson type III distributions.
- The IDF equation for Gumbel's distribution is most reliable for the catchment as it has the highest R² value (0.9865) compared to Pearson type (III) and Log-Pearson type (III), which are 0.9766 and 0.982, respectively.
- There was no significant difference between the rainfall intensities predicted from all the IDF equations and those observed in the field, based on t-test analysis ($p < 0.01$).
- The Sherman's regional constants c , m , and e for the catchment are 503.96, 0.1664, and 0.66686 for Gumbel; 517.37, 0.1546, and 0.6669 for Pearson type (III); 510.62, 0.1616 and 0.66688 for Log-Pearson type (III) correspondingly.

ABSTRACT

Hydraulic structures such as surface drainages and culverts are usually constructed in urban areas to drain runoff into nearby streams and rivers to avoid flooding. However, most of these structures frequently fail to serve the intended use due to high-intensity rainfall accompanied by long duration, which produces runoff discharge higher than their designed capacities. This is common in many developing countries as drainages and culverts are usually constructed without considering the catchment's hydrological analysis. Hence, this research considered Port Harcourt city as a case study by utilizing 50 years of rainfall data to develop rainfall Intensity-Duration-Frequency (IDF) curves used for the subsequent design of drainages and culverts within the city and its environs. The IDF curves were developed using Gumbel, Pearson type III, and Log-Pearson type III distributions at return periods of 2, 5, 10, 25, and 50years. However, the durations considered were 5, 10, 20, 30, 45, 60, 90, 120, 150, 180, 210, 240, 300, 360 and 420minutes. Results showed that the IDF equations developed for the three frequency distributions highly correlate with the observed intensities since their goodness of fit (R²) ranges from 0.9766 to 0.9865. Also, it was noted that there was no significant difference ($p < 0.01$) between the predicted rainfall intensities from all the IDF equations and the observed intensities. Notwithstanding, the IDF equation developed for Gumbel distribution was recommended to be given higher priority since it has the highest R² value.

ARTICLE INFO

Handling editor: Wasan I. Khalil

Keywords: Gumbel, Pearson type III, Log-Pearson type III, Return-Period, Port Harcourt.

1. Introduction

Hydraulic structures such as bridges, culverts, drainages, and dams, are usually designed to serve for a certain period. However, the structures often fail to serve the intended purpose in certain years within the designed period due to excessive flood, runoff, or high stream flow rates, which all depend on rainfall. This has been recorded in different parts of the world, especially in developing countries like Nigeria. For instance, the collapse of the Tatabu bridge along Mokwa-Jebba road in Niger state of Nigeria in 2017 was attributed to the increase in rainfall between 2015 and 2017, which directly increased the runoff and streamflow rate [1]. Furthermore, past research conducted in Nigeria [2] revealed that several bridges failed due to floods, as shown in Table 1.

Port Harcourt, the capital of Rivers state in South-Southern Nigeria, has been experiencing annual floods significantly [3]. Although urban flooding could be caused by several factors notwithstanding, the lack of a good surface drainage network system is a key factor. The procedure for constructing surface drainages requires a geological survey of the site, hydrological analysis, hydraulic design, and structural drainage analysis. However, in most developing countries, hydrological analysis requires numerous data, such as previous rainfalls, to determine rainfall intensity at a given return period and duration. Surface runoff and concentration-time are not usually considered due to a lack of experts and field data. In fact, most of the few rain gauges installed in certain cities in developing countries are not automated; hence the amount of depth of rainfall is recorded manually by reading the values in the gauge at a regular interval within 24hours (either 6, 12, or 24hours interval). In other words, getting field data for hydrological analysis is a big challenge facing most developing countries. This was earlier identified by a previous researcher who ascribed the issue of flooding in Port Harcourt to culvert inadequacy due to insufficient or lack of field data used in design [4]. This affects the hydraulic design for optimal or most economical sections of drainages, thus, causing surface drainage systems to be unable to contain future torrential rainfall, which would have been easily handled if reliable rainfall IDF models of the catchment were available. Notwithstanding, the rainfall IDF models for Port Harcourt have earlier been developed on two occasions by [5, 6]. However, the data employed on both occasions were insufficient. The former used 10 years (1970 – 1979) rainfall data while the latter utilized 16 years (1998 – 2013) rainfall data to develop the rainfall IDF models of the said area. Since rainfall IDF models are used to predict rainfall intensities for return periods as high as 50 years and beyond, it requires a minimum of 30 years of rainfall data to establish such models based on the conventional standard. Hence, this research utilized 50 years (1971 – 2020) rainfall data to establish rainfall IDF models for Port Harcourt to be compared and used alongside earlier developed ones.

2. Materials and Methods

2.1 Description of Study Area

Port Harcourt is located in Southern Nigeria, and it is the capital of Rivers State and the largest city in the state. It comprises two Local Government Areas (LGA) known as Port Harcourt city LGA and Obio-Akpor LGA (Figure 1), all enclosed in between Latitude 4° 42' 00" to 40 57' 03" North and Longitude 6° 53' 11" to 70 8' 49" East with an approximate area of 369km². The peak daily rainfall in the study area for the past 50years mostly occurs between June to October.

The first meteorological station in the study area was established in 1965 at the Airforce Base (Latitude 4° 50' 53.89" North; Longitude 7° 1' 17.87" East) along Port Harcourt – Aba road. However, the Nigerian civil war that lasted for 30months (July 1967 to January 1970) led to the missing rainfall data during this period since the rainfall depths were recorded manually from the rain gauge. Notwithstanding, the meteorological station commenced operations again between 1970 to 1979 but moved to the Port Harcourt International Airport Omagwa (Latitude 5° 0' 54.58" North; Longitude 6° 57' 14.69" East) in 1980, and it has remained there since then.

2.2 Data Collection and Analysis

Beginning from the year 1971 to 2020 (50years), the highest or maximum daily rainfall depth (mm) for each year in Port Harcourt was obtained from the headquarters of the Nigerian Meteorological Agency (NIMET) Abuja. Since the daily (24hours) rainfall depths were manually recorded, the maximum rainfall depths corresponding to shorter durations (5, 10, 20, 30, 45, 60, 90, 120, 150, 180, 210, 240, 300, 360, and 420minutes) for each year were determined by employing the empirical model developed by the Indian Meteorological Department (IMD) shown in Equation (1) as follows.

$$P_t = P_{24} \left(\frac{t}{24} \right)^{1/3} \quad (1)$$

Where P_t is the required precipitation depth in mm for t -hours, P_{24} is the annual maximum daily (24hours) rainfall depth in mm, and t is the duration in hours for the required precipitation depth. The rainfall intensities (I) in mm/hour for the different durations were obtained by dividing the rainfall depths in mm by their corresponding durations in hours. The intensities (I) obtained for the various durations were ranked in descending order ($m = 1$ for highest intensity). After that, the frequencies (return periods) of the various storms were calculated using Weibull's method, as shown in Equation (2).

Table 1: Some collapsed bridges in Nigeria were caused by flood

Name of Bridge	State	Location	Year
Mararraban Gassol Bembal bridge	Taraba	Wukari-Jalingo road	2018
Gulbim Boka bridge	Niger	Mariga	2018
Eme bridge	Abia	Amoji-Imenyi, Bende	2017
Bebuo Bomaji bridge	Cross River	Bebuo Bomaji, Boki	2017
Idi-Iroko bridge	Osun	Iwo	2017
Pandaragi bridge	Kwara	Pandaragi	2017
Alagbado bridge	Kwara	Ilorin East	2017
Chibiri bridge	Plateau	Langkaku, Qua'an Pan	2016
Dubban Fulani bridge	Gombe	Dubban fulani, Debba	2015
Odo pako bridge	Ogun	Agbado	2013
Yar'randa bridge	Katsina	Yar'randa, Charanchi	2013
Imiringi bridge	Bayelsa	Imiringi, Ogbia	2012

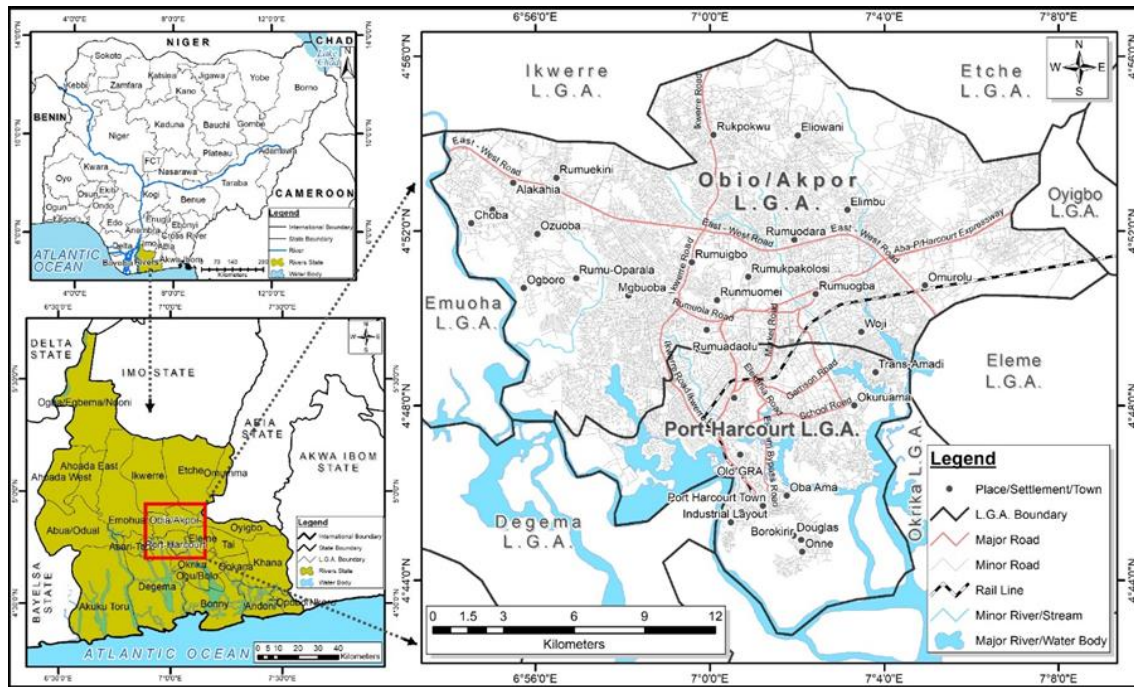


Figure 1: Map of the study area

(Source: Modified from <https://www.openstreetmap.org/#map=6/9.117/8.674>)

$$T = \frac{n+1}{m} \quad (2)$$

Where T is the frequency or return period, n is the number of years of recorded data (50), and m is the rank. For example, the t return period for urban drainage and culvert designs within the region (Nigeria) is usually 25 years. Still, to develop IDF equations for the catchment, other return periods apart from 25, present in standard frequency or return period Tables were considered. Hence, this research considered return periods 2, 5, 10, 25, and 50 years.

The intensities for each return period were plotted against their respective durations on a linear graph.

Gumbel, Pearson type III, and Log-Pearson type III, which are the most commonly used IDF curves, were developed for the catchment by means of the general hydrologic frequency distribution model given in Equation (3).

$$X_T = \bar{X} + K_T \sigma \quad (3)$$

Where X_T is the rainfall intensity for a return period T , \bar{X} is the arithmetic mean of rainfall intensity for a given storm duration, σ is the standard deviation of rainfall intensity for a given storm duration while K_T is the frequency factor, which is a function of return period T . The frequency factor K_T for Gumbel's distribution was determined utilizing Equation (4) as follows;

$$K_T = -\frac{\sqrt{6}}{\pi} \left[0.5772 + \ln \left(\ln \frac{T}{T-1} \right) \right] \quad (4)$$

Where T is the return period.

The Pearson type III distribution is usually suitable for skewed data; hence the K_T factor also depends on the coefficient of skewness which was determined using Equation (5).

$$C_s = \frac{n \sum_{i=1}^n (X_{i=1} - \bar{X})^3}{(n-1)(n-2)\sigma^3} \quad (5)$$

Where C_s is coefficient of skewness, n is the number of years of recorded data (sample size = 50), X_i is the individual or yearly rainfall intensity for a given duration, \bar{X} is the arithmetic mean of rainfall intensity for a given duration, σ is the standard deviation of rainfall intensity for a given duration. Hence, the frequency factor K_T for Pearson type III distribution for a given return period was obtained from the standard Table using the determined coefficient of skewness.

The frequency factor K_T for Log-Pearson type III distribution was obtained similarly as in the case of Pearson type III distribution. However, the rainfall intensities were logarithmically transformed to base 10. In other words, the arithmetic mean and standard deviation of the rainfall intensities were calculated based on the logarithmically transformed data and were used to determine the skewness coefficient. After that, the frequency factor K_T for a given return period was obtained from a standard Table using the determined skewness coefficient. Hence, the calculated logarithmically transformed mean, standard

deviation, and frequency factor K_T for each duration for a given return period were substituted into Equation (3) to obtain the corresponding log-transformed rainfall intensities. Thus, the solutions obtained in Equation (3), i.e., antilog of log-transformed rainfall intensities, give the actual rainfall intensities of the various rainfall durations and return periods.

2.3 Derivation of IDF Equations

The general equation relating the dependent variable (rainfall intensity) and the independent variables (rainfall duration and return period or frequency) governing each frequency distribution (Gumbel, Pearson type III, and Log-Pearson type III) curve was determined using Sherman's model shown in Equation (6).

$$i = \frac{cT^m}{t^e} \quad (6)$$

Where i is the rainfall intensity in mm/hr, T is the frequency or return period in years, t is the rainfall duration in minutes, while c , m , and e are constants depending on the region or catchment. The procedure used in determining these regional constants (c , m , and e) are as follows;

Equation (6) was linearized logarithmically, as shown in Equation (7).

$$\log i = -e \log t + \log K \quad (7)$$

Where K is expressed in Equation (8)

$$K = cT^m \quad (8)$$

Equation (7) was applied to the data for each frequency distribution (Gumbel, Pearson type III, and Log-Pearson type III) at a given return period T by plotting values of $\log i$ (on the y-axis) against $\log t$ (on the x-axis) using a linear graph. The slope or gradient of the graph was taken as the constant e for the return period considered. The arithmetic mean of the various e (slopes) values resulting from each return period was calculated and taken as the regional constant e for Equation (7). Also, the y-intercepts of the graphs plotted were taken as the values of $\log K$ (where $K = cT^m$) for their corresponding return period T . To determine the regional constants c and m , Equation (8) was also linearized as shown in Equation (9).

$$\log K = m \log T + \log c \quad (9)$$

Hence, Equation (9) was applied to the data for the various frequency distributions by plotting the various values of $\log K$ (already determined as y-intercepts of the graphs of Equation 7) against the log of their corresponding return periods T on a linear graph. Thus, the slope of the graph obtained represents the constant m while the y-intercept was taken as $\log c$. Hence the actual value of constant c was determined by obtaining the antilog of the y-intercept of the Equation (9) graph.

The constants c , m , and e obtained for Gumbel, Pearson type III, and Log-Pearson type III distribution functions were substituted into Sherman's IDF model presented in Equation (6) as the general IDF equation for the catchment for the considered frequency distribution functions.

To decide the best IDF equation, a correlation analysis was carried out between the original rainfall intensities (observed data) and the rainfall intensities obtained through the IDF equations (predicted data). The one with the highest determination coefficient (R²) value was considered the IDF equation that best suits the catchment.

3. Results and Discussion

3.1 Results

The original rainfall intensities for the various durations are ranked as shown in Table 2.

3.1.1 Gumbel's distribution

The frequency factor (K_T) for Gumbel's distribution for the various return periods 2, 5, 10, 25, and 50 were obtained from Equation (4) as -0.1643 , 0.7194 , 1.3044 , 2.0436 , and 2.5919 , respectively. The mean (\bar{X}) and standard deviation (σ) values corresponding to various storm durations in Table 2, together with the computed K_T values were substituted in Equation (3) to generate the corresponding rainfall intensities for Gumbel's distribution, shown in Table 3 and Figure 2.

3.1.2 Pearson type III distribution

The skewness coefficients (C_s) of the various durations shown in Table 2 lies between 0.6 and 0.8; hence, the frequency factor (K_T) for each return period corresponding to the computed skewness coefficient were interpolated between 0.6 and 0.8 from standard Pearson type (III) Table. The obtained interpolated K_T values alongside the mean (\bar{X}) and standard deviation (σ) values corresponding to the various durations in Table 2 were substituted into Equation (3) to generate the rainfall intensity values presented in Table 4. The intensities values in Table 4 were used in producing the IDF curves in Figure 3.

3.1.1 Log-Pearson type (III) distribution

The intensity values shown in Table 2 were logarithmically transformed to obtain the log-transformed mean, standard deviation, and skewness coefficient for each duration. The corresponding transformed frequency factors (K_T) were obtained in standard Table by interpolation just as in the case of Pearson type (III). The obtained log-transformed mean (\bar{X}), standard deviation (σ) and frequency factor (K_T) for the various durations and considered return periods were substituted into Equation (3) to yield log-transform intensity values. The actual intensity values, which are the antilog of the log-transformed intensities, are shown in Table 5, while the corresponding IDF curves are shown in Figure 4.

Table 2: Rainfall intensities (mm/h) for short durations computed from observed daily rainfall

Rank <i>m</i>	5 min.	10 min.	20 min.	30 min.	45 min.	60 min.	90 min.	120 min.	150 min.	180 min.	210 min.	240 min.	300 min.	360 min.	420 min.
1*	337.	211.	133.	101.											
	8	7	7	9	77.8	64.3	49.0	40.5	34.9	30.9	27.9	25.5	22.0	19.5	17.6
2*	316.	198.	125.												
	1	1	1	95.4	72.8	60.1	45.9	37.9	32.6	28.9	26.1	23.9	20.6	18.2	16.4
3	297.	186.	117.												
	0	1	5	89.6	68.4	56.5	43.1	35.6	30.7	27.2	24.5	22.4	19.3	17.1	15.4
4	259.	162.	102.												
	4	6	7	78.3	59.8	49.4	37.7	31.1	26.8	23.7	21.4	19.6	16.9	14.9	13.5
5*	258.	161.	102.												
	0	7	1	77.8	59.4	49.1	37.4	30.9	26.6	23.6	21.3	19.5	16.8	14.9	13.4
6	243.	152.													
	9	9	96.5	73.6	56.2	46.4	35.4	29.2	25.2	22.3	20.1	18.4	15.9	14.0	12.7
7	243.	152.													
	2	4	96.2	73.4	56.0	46.3	35.3	29.1	25.1	22.2	20.1	18.4	15.8	14.0	12.6
8	242.	151.													
	1	7	95.8	73.1	55.8	46.1	35.1	29.0	25.0	22.1	20.0	18.3	15.7	13.9	12.6
9	240.	150.													
	3	6	95.1	72.5	55.4	45.7	34.9	28.8	24.8	22.0	19.8	18.1	15.6	13.8	12.5
10*	236.	148.													
	3	1	93.5	71.3	54.4	44.9	34.3	28.3	24.4	21.6	19.5	17.8	15.4	13.6	12.3
11	234.	146.													
	3	8	92.7	70.7	54.0	44.6	34.0	28.1	24.2	21.4	19.3	17.7	15.2	13.5	12.2
12	234.	146.													
	1	7	92.6	70.6	53.9	44.5	34.0	28.0	24.2	21.4	19.3	17.7	15.2	13.5	12.2
13	231.	144.													
	0	7	91.4	69.7	53.2	43.9	33.5	27.7	23.9	21.1	19.1	17.4	15.0	13.3	12.0
14	229.	143.													
	5	8	90.8	69.3	52.9	43.7	33.3	27.5	23.7	21.0	18.9	17.3	14.9	13.2	11.9
15	224.	140.													
	0	4	88.7	67.6	51.6	42.6	32.5	26.8	23.1	20.5	18.5	16.9	14.6	12.9	11.6
16	217.	136.													
	7	4	86.1	65.7	50.2	41.4	31.6	26.1	22.5	19.9	18.0	16.4	14.2	12.5	11.3
17	217.	136.													
	7	4	86.1	65.7	50.2	41.4	31.6	26.1	22.5	19.9	18.0	16.4	14.2	12.5	11.3
18	215.	134.													
	3	9	85.2	65.0	49.6	41.0	31.2	25.8	22.2	19.7	17.8	16.3	14.0	12.4	11.2
19	210.	131.													
	2	7	83.2	63.4	48.4	40.0	30.5	25.2	21.7	19.2	17.3	15.9	13.7	12.1	10.9
20	205.	128.													
	1	5	81.2	61.9	47.3	39.0	29.8	24.6	21.2	18.8	16.9	15.5	13.3	11.8	10.7
21	202.	127.													
	9	2	80.3	61.2	46.7	38.6	29.4	24.3	21.0	18.6	16.7	15.3	13.2	11.7	10.5
22	197.	123.													
	3	6	78.1	59.5	45.4	37.5	28.6	23.6	20.4	18.0	16.3	14.9	12.8	11.4	10.3
23	190.	119.													
	1	2	75.3	57.4	43.8	36.2	27.6	22.8	19.6	17.4	15.7	14.4	12.4	11.0	9.9
24	189.	118.													
	2	6	74.9	57.1	43.6	36.0	27.5	22.7	19.5	17.3	15.6	14.3	12.3	10.9	9.8
25	188.	118.													
	7	2	74.7	56.9	43.5	35.9	27.4	22.6	19.5	17.3	15.6	14.2	12.3	10.9	9.8
26*	188.	117.													
	0	8	74.4	56.7	43.3	35.8	27.3	22.5	19.4	17.2	15.5	14.2	12.2	10.8	9.8
27	183.	114.													
	2	8	72.5	55.3	42.2	34.9	26.6	21.9	18.9	16.8	15.1	13.8	11.9	10.6	9.5
28	180.	113.													
	7	2	71.5	54.5	41.6	34.4	26.2	21.6	18.7	16.5	14.9	13.6	11.7	10.4	9.4
29	179.	112.													
	6	5	71.1	54.2	41.4	34.2	26.1	21.5	18.5	16.4	14.8	13.6	11.7	10.3	9.3
30	178.	111.													
	5	8	70.6	53.9	41.1	34.0	25.9	21.4	18.4	16.3	14.7	13.5	11.6	10.3	9.3
31	178.	111.													
	3	7	70.6	53.8	41.1	33.9	25.9	21.4	18.4	16.3	14.7	13.5	11.6	10.3	9.3
32	177.	111.													
	6	3	70.3	53.6	40.9	33.8	25.8	21.3	18.3	16.2	14.6	13.4	11.5	10.2	9.2
33	175.	110.													
	6	0	69.5	53.0	40.4	33.4	25.5	21.0	18.1	16.1	14.5	13.3	11.4	10.1	9.1
34	171.	107.													
	0	2	67.7	51.6	39.4	32.5	24.8	20.5	17.7	15.6	14.1	12.9	11.1	9.8	8.9
35	170.	106.													
	6	9	67.5	51.5	39.3	32.5	24.8	20.4	17.6	15.6	14.1	12.9	11.1	9.8	8.9

Table 2: : Continued

Rank <i>m</i>	5 min.	10 min.	20 min.	30 min.	45 min.	60 min.	90 min.	120 min.	150 min.	180 min.	210 min.	240 min.	300 min.	360 min.	420 min.
36	169.	106.													
	9	5	67.2	51.3	39.1	32.3	24.7	20.4	17.5	15.5	14.0	12.8	11.1	9.8	8.8
37	169.	106.													
	4	1	67.0	51.1	39.0	32.2	24.6	20.3	17.5	15.5	14.0	12.8	11.0	9.8	8.8
38	157.														
	0	98.4	62.1	47.4	36.2	29.9	22.8	18.8	16.2	14.4	12.9	11.8	10.2	9.0	8.2
39	151.														
	9	95.2	60.1	45.8	35.0	28.9	22.0	18.2	15.7	13.9	12.5	11.5	9.9	8.7	7.9
40	147.														
	5	92.4	58.4	44.5	34.0	28.1	21.4	17.7	15.2	13.5	12.2	11.1	9.6	8.5	7.7
41	146.														
	8	92.0	58.1	44.3	33.8	27.9	21.3	17.6	15.2	13.4	12.1	11.1	9.5	8.5	7.6
42	146.														
	4	91.7	57.9	44.2	33.7	27.8	21.2	17.5	15.1	13.4	12.1	11.0	9.5	8.4	7.6
43	146.														
	4	91.7	57.9	44.2	33.7	27.8	21.2	17.5	15.1	13.4	12.1	11.0	9.5	8.4	7.6
44	140.														
	0	87.7	55.4	42.2	32.3	26.6	20.3	16.8	14.5	12.8	11.5	10.6	9.1	8.1	7.3
45	136.														
	4	85.5	54.0	41.1	31.4	25.9	19.8	16.3	14.1	12.5	11.2	10.3	8.9	7.9	7.1
46	132.														
	0	82.7	52.2	39.8	30.4	25.1	19.2	15.8	13.6	12.1	10.9	10.0	8.6	7.6	6.9
47	129.														
	4	81.1	51.2	39.1	29.8	24.6	18.8	15.5	13.4	11.8	10.7	9.8	8.4	7.5	6.7
48	127.														
	6	80.0	50.5	38.5	29.4	24.3	18.5	15.3	13.2	11.7	10.5	9.6	8.3	7.3	6.6
49	125.														
	4	78.6	49.6	37.8	28.9	23.9	18.2	15.0	13.0	11.5	10.3	9.5	8.2	7.2	6.5
50	122.														
	3	76.7	48.4	36.9	28.2	23.3	17.8	14.7	12.6	11.2	10.1	9.2	8.0	7.0	6.4
\bar{X}	195.	122.													
	8	7	77.5	59.1	45.1	37.3	28.4	23.5	20.2	17.9	16.2	14.8	12.7	11.3	10.2
σ	49.3	30.9	19.5	14.9	11.3	9.4	7.1	5.9	5.1	4.5	4.1	3.7	3.2	2.8	2.6
C_s	0.73	0.73	0.73	0.72	0.75	0.71	0.76	0.71	0.74	0.74	0.68	0.72	0.77	0.74	
	5	5	5	8	0	3	0	4	2	0	2	9	3	0	0.676

* represent ranks corresponding to considered return periods (i.e. rank $m = 1, 2, 5, 10$ and 26 correspond to return periods $50, 25, 10, 5$ and 2 years respectively).

Table 3: Gumbel's distribution rainfall intensity (mm/hr) for considered return periods

Rank <i>m</i>	5 min.	10 min.	20 min.	30 min.	45 min.	60 min.	90 min.	120 min.	150 min.	180 min.	210 min.	240 min.	300 min.	360 min.	420 min.	$T = \frac{n+1}{m}$
26	187.	117.						22.								2
	8	7	74.3	56.7	43.3	35.7	27.3	5	19.4	17.2	15.5	14.2	12.2	10.8	9.8	
10	231.	144.						27.								5
	3	9	91.5	69.8	53.3	44.0	33.6	7	23.9	21.1	19.1	17.5	15.0	13.3	12.0	
5	260.	163.						31.								10
	1	0	9	78.5	59.9	49.5	37.8	2	26.9	23.8	21.5	19.6	16.9	15.0	13.5	
2	296.	185.						35.								25
	5	8	3	89.5	68.3	56.4	43.0	5	30.6	27.1	24.5	22.4	19.3	17.1	15.4	
1	323.	202.						38.								50
	6	8	0	97.7	74.4	61.7	46.8	8	33.4	29.6	26.8	24.4	21.0	18.6	16.9	

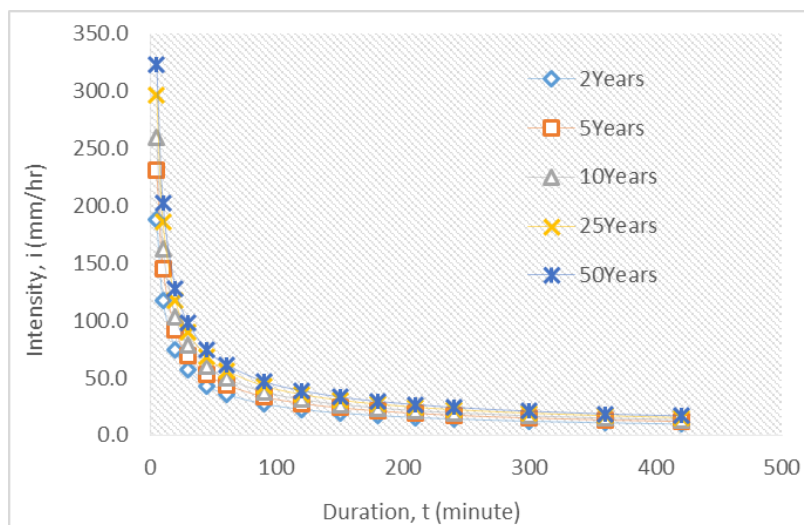


Figure 2: IDF curves for Gumbel's distribution

Table 4: Pearson type (III) rainfall intensities (mm/hr) for considered return periods

Rank <i>m</i>	5 min.	10 min.	20 min.	30 min.	45 min.	60 min.	90 min.	120 min.	150 min.	180 min.	210 min.	240 min.	300 min.	360 min.	420 min.	$T = \frac{n+1}{m}$
26	189.9	119.0	75.1	57.3	43.7	36.2	27.5	22.8	19.6	17.4	15.7	14.3	12.3	10.9	9.9	2
10	234.6	147.0	92.8	70.8	54.0	44.6	34.0	28.1	24.2	21.4	19.4	17.7	15.2	13.5	12.2	5
5	261.5	163.9	103.5	78.9	60.3	49.7	38.0	31.3	27.0	23.9	21.6	19.7	17.0	15.1	13.6	10
2	293.2	183.7	116.0	88.4	67.6	55.7	42.6	35.1	30.3	26.8	24.1	22.1	19.1	16.9	15.2	25
1	315.2	197.5	124.7	95.1	72.7	59.9	45.8	37.7	32.6	28.8	25.9	23.8	20.6	18.2	16.3	50

Table 5: Log-Pearson type (III) rainfall intensities (mm/hr) for considered return periods

Rank <i>m</i>	5 min.	10 min.	20 min.	30 min.	45 min.	60 min.	90 min.	120 min.	150 min.	180 min.	210 min.	240 min.	300 min.	360 min.	420 min.	$T = \frac{n+1}{m}$
26	189.0	118.4	74.8	57.1	43.5	35.9	27.4	22.6	19.5	17.3	15.6	14.3	12.3	10.9	9.8	2
10	233.3	146.2	92.3	70.4	53.8	44.4	33.9	27.9	24.1	21.3	19.2	17.6	15.2	13.4	12.1	5
5	261.5	163.9	103.5	78.9	60.3	49.8	37.9	31.3	27.0	23.9	21.6	19.7	17.0	15.1	13.6	10
2	295.8	185.3	117.1	89.2	68.2	56.3	42.9	35.5	30.5	27.0	24.4	22.3	19.2	17.0	15.4	25
1	320.7	201.0	127.1	96.6	74.0	61.1	46.5	38.5	33.1	29.3	26.5	24.2	20.9	18.5	16.6	50

Table 6: Regional constants and IDF equations of the catchment for considered distributions

Distribution	<i>c</i>	<i>m</i>	<i>e</i>	$i = \frac{cT^m}{t^e}$	R^2
Gumbel	503.96	0.1664	0.66686	$i = \frac{503.96T^{0.1664}}{t^{0.66686}}$	0.9865
Pearson Type (III)	517.37	0.1546	0.6669	$i = \frac{517.37T^{0.1546}}{t^{0.6669}}$	0.9766
Log-Pearson Type (III)	510.62	0.1616	0.66688	$i = \frac{510.62T^{0.1616}}{t^{0.66688}}$	0.982

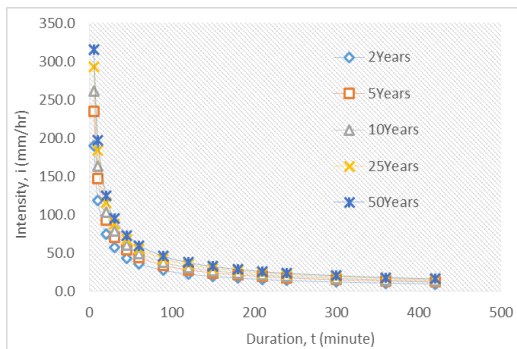
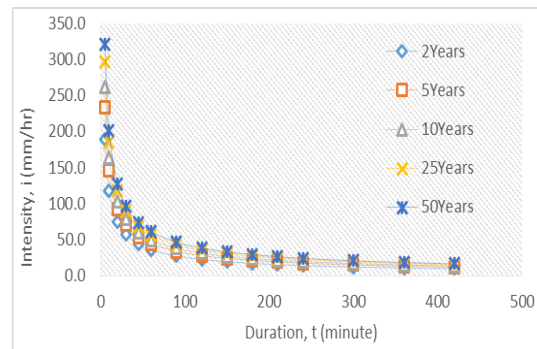
i = Rainfall intensity in mm/hr, T = return period in years, t = duration in minute, R^2 = determination coefficient, while c , m and e are regional constants.

3.1.2 IDF equations

The regional constant e in Sherman's model was determined for Gumbel's distribution by plotting the log of rainfall intensity ($\log i$) against the log of their corresponding duration ($\log t$) for each return period, as shown in Figure 5.

The regression lines associated with the various plots shown in Figure 5 were compared with Equation (7), and the average value of the constant e was obtained (0.66686). The associated y-intercepts of the various plots in Figure 5, which represent $\log K$ (based on Equation 7), were plotted against the log of their corresponding return period ($\log T$) as shown in Figure 6. The regression equation for the curve in Figure 6 was compared with Equation (9). The regional constant m for Gumbel's distribution was determined from the gradient of the curve displayed in Figure 6 (i.e., 0.1664). Also, by comparing Equation (9) with the regression equation in Figure 6, it is glaring that the regional constant c is equivalent to the antilog of the y-intercept of the curve in Figure 6. (i.e. $10^{2.7024} = 503.96$).

The regional constants c , m , and e for Pearson type (III) and Log-Pearson type (III) distributions were determined similarly. They were substituted into Equation (6) to obtain the IDF equation of the catchment for each distribution, as shown in Table 6. Then, the determined IDF equations were used to generate predicted rainfall intensities for the various durations in each return period, which were correlated with the observed rainfall intensities. The coefficients of determination (R^2) of the correlation in each frequency distribution are shown in Table 6.

**Figure 3:** IDF curves for Pearson type (III) distribution**Figure 4:** IDF curves for Log-Pearson type (III) distribution

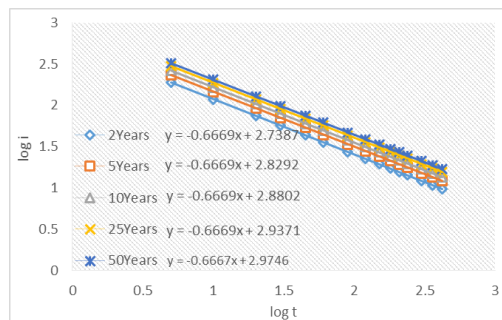


Figure 5: Determination of regional constant e for Gumbel's distribution

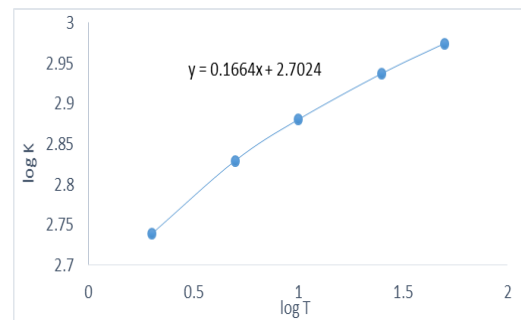


Figure 6: Determination of regional constants c and m for Gumbel's distribution

3.2 Discussion

The curves in Figures 2, 3, and 4 revealed that high-intensity rainfalls had shorter durations, which is a basic principle in hydrology. It was also noted that the intensities increase with the return period, which is in line with previous related research [7-11]. Gumbel's distribution predicted the same rainfall intensities with the observed data for the various durations during 2years return period, while Pearson type (III) and Log-Pearson type (III) predicted rainfall intensities slightly higher than the observed values during 2years return period. However, all the frequency distributions considered predicted rainfall intensities slightly lower than the observed rainfall intensities during 5years, 25, and 50years return periods but slightly higher than observed intensities during the 10 years return period. Notwithstanding, there was no significant difference between the rainfall intensities predicted from all the IDF equations and those observed or recorded in the field, based on t-test analysis ($p < 0.01$). Also, the correlation between the predicted intensities generated from these models (equations) and the observed intensities fitted well in their respective regression lines, with high R^2 values ranging from 0.9766 to 0.9865. In other words, the IDF equations developed to predict rainfall intensities of the catchment at any given return period and duration were highly reliable for all the frequency distributions considered (Gumbel, Pearson type III, and Log-Pearson type III). Nevertheless, the IDF equation for Gumbel's distribution is most reliable for the catchment as it has the highest R^2 value (0.9865) compared to Pearson type (III) and Log-Pearson type (III), which are 0.9766 and 0.982, respectively. Earlier research conducted in this catchment also revealed that Gumbel's distribution is more reliable than Pearson type (III) and Log-Pearson type (III) distribution for the catchment [6].

The Sherman's regional constants c , m , and e for the catchment area 503.96, 0.1664, and 0.66686 for Gumbel; 517.37, 0.1546, and 0.6669 for Pearson type (III); 510.62, 0.1616 and 0.66688 for Log-Pearson type (III) correspondingly. These values negate the assertion of a past work done in the catchment as it reports the regional constants c , m , and e for the same catchment as 416.54, 0.2412, and 0.5613 for Gumbel; 479.458, 0.230, and 0.600 for Pearson type (III); 481.679, 0.300 and 0.654 for Log-Pearson type (III) in that order [6]. The discrepancy could be attributed to the difference in the rainfall data sample size since this research used 50years (1971 – 2020) rainfall data while the other utilized just 16years (1998 – 2013) data.

4. Conclusion and Recommendations

The research has provided highly reliable IDF equations that could predict the rainfall intensities of Port Harcourt at different durations and return periods using Gumbel, Pearson type (III), and Log-Pearson type (III) distributions. Hence, it is recommended that the developed IDF models be used when designing hydraulic structures such as surface drainages and culverts within Port Harcourt city and its environs to minimize the flooding usually experienced in the city. However, priority should be given to the IDF equation developed for Gumbel's distribution since it has the best goodness of fit when correlated with observed data. It is also recommended that the Nigerian Meteorological Agency (NIMET) install automatic rain-gauge stations within Port Harcourt city.

Author contribution

author contributed equally to this work.

Funding

This research received no specific grant from any funding agency in the public, commercial, or not-for-profit sectors.

Data availability statement

The data that support the findings of this study are available on request from the corresponding author.

Conflicts of interest

The authors declare that there is no conflict of interest.

References

- [1] J. Sule, I.A. Inuwa, S.L. Abdulahi, and D.S. Matawal, Bridge Collapse in Nigeria: A Case Study of Tatabu Bridge in Mokwa Local Government Area of Niger State, *Civil Engineering Research*, 10 (2018) 39-51.
- [2] A. Ede, C.O. Nwankwo, S. Oyebisi, O. Olofinnade, A. Okeke, and A. Busari, Failure Trend of Transport Infrastructure in Developing Nations: Case of Bridges Collapse in Nigeria, *The 1st International Conference on Sustainable Infrastructural Development: Material Science and Engineering Series*, Canan Land-Ota, 2019. doi:10.1088/1757-899X/640/1/012102.
- [3] A.J. Echendu, Relationship between Urban Planning and Flooding in Port Harcourt City, Nigeria; Insights from Planning Professionals, *Journal of Flood Risk Management*, 14 (2021) 1-13, <https://doi.org/10.1111/jfr3.12693>.
- [4] I.L. Nwaogazie, and G.C. Agiho, Performance Analysis of Box and Circular Culverts Using HY 8 Software for Aluu Clan, Port Harcourt, *Nigerian Journal of Technology*, 38 (2019) 22-32.
- [5] I.L. Nwaogazie, and E.O. Duru, Development of Rainfall-Intensity-Duration-Frequency Models for Port Harcourt City, *NSE Technical Transaction*, 37 (2002) 19-32.
- [6] I.L. Nwaogazie, and M.G. Sam, Probability and Non-Probability Rainfall Intensity-Duration-Frequency Modeling for Port-Harcourt Metropolis, Nigeria, *International Journal of Hydrology*, 3 (2019) 66-75.
- [7] A. Mohammed, S.D. Azumi, A.A. Modibbo, and A.A. Adamu, Development of Rainfall Intensity Duration Frequency (IDF) Curves for Design of Hydraulic Structures in Kano State, Nigeria, *Platform-A Journal of Engineering*, 5 (2021) 10-22.
- [8] A.R. Majeed, B.K. Nile, and J.H. Al-Baidhani, Selection of Suitable PDF Model and Build of IDF Curves for Rainfall in Najaf City, Iraq, *Journal of Physics: Conference Series* 1973 (2021) 1-13, 2021. doi:10.1088/1742-6596/1973/1/012184.
- [9] Agarwal, S., Kumar, S. and Singh, U.K. Intensity Duration Frequency Curve Generation Using Historical and Future Downscaled Rainfall Data. *Indian Journal of Ecology*, 48 (2021) 275-280.
- [10] A.S. Al-Wagdany, Intensity-Duration-Frequency Curve Derivation from Different Rain Gauge Records, *Journal of King Saud University-Science*, 32 (2020) 3421-3431.
- [11] T. Gratein, M.J. Kundwa, P. Bakunzibake, P. Bunani, and J.L. Habyarimana, Development of Rainfall Intensity Duration Frequency (IDF) Curves for Hydraulic Design Aspect, *Journal of Ecology and Natural Resources*, 3 (2019) 1-14.